

## Growth Processes of $\text{Cu}_2\text{ZnSn}(\text{S}_{1-x}\text{Se}_x)_4$ -Au Nanocomposites: Microanalysis and Corresponding Impacts on Photovoltaic Properties

Shuai Ma<sup>1</sup>, Jie Wang<sup>2</sup>, Fengjin Xia<sup>1</sup>, Yingjie Chen<sup>2</sup>, Hongzhou Dong<sup>2</sup>, Liyan Yu<sup>2</sup> and Lifeng Dong<sup>2, 3</sup>

<sup>1</sup> School of Mathematics & Physics, Qingdao University of Science and Technology, Qingdao 266061, PR China

<sup>2</sup> College of Materials Science & Engineering, Qingdao University of Science and Technology, Qingdao 266042, PR China

<sup>3</sup> Department of Physics, Hamline University, St. Paul 55104, USA

Colloidal  $\text{Cu}_2\text{ZnSn}(\text{S}_{1-x}\text{Se}_x)_4$  (CZTSSe for  $0 < x < 1$ , and CZTS if  $x = 0$ ) has been regarded as emerging direct-bandgap semiconductor, providing potentiality for large-scale photovoltaic manufacture [1]. Au nanoparticles can generate electric-field enhancement at their surfaces due to localized surface plasmon resonances (LSPR) effects [2]. Designing nano-heterostructures of CZTSSe coupling with noble metal particles could help to develop novel plasmon-enhanced photovoltaic/photocatalytic materials [3]. Crystallographic analysis of  $\text{Cu}_2\text{ZnSn}(\text{S}_{1-x}\text{Se}_x)_4$  nanoparticles has been reported in our previous work [4]. In this work, we mainly explore growth processes of Au nanoparticles at  $\text{Cu}_2\text{ZnSn}(\text{S}_{1-x}\text{Se}_x)_4$  in order to obtain valuable information on the correlations between photovoltaic performance and nanocomposite structures.

In our experiments, CZTS and CZTSSe nanoparticles were synthesized by hot-injection method. Diluted  $\text{HAuCl}_4 \cdot 3\text{H}_2\text{O}$  (0.25 mL) was heated to boiling and mixed with sodium citrate and citric acid. After stirring, the reactant with Au particles was dropwise added into prepared CZTS/CZTSSe solution, and then the methanol was immediately added for precipitating. The detailed synthesis protocols were reported in our previous work [4]. The microstructures of products were examined by high resolution transmission electron microscopy (HRTEM, JEM2100 with 200 kV accelerating voltage).

A wide view of synthesized CZTS-Au nanocomposites (Figure 1a) reveals that multiple Au nanocrystals with a diameter of circa 2 nm evenly distribute on the surface of CZTS particles with a size distribution ranging from 10 nm to 15 nm; while Au nanocrystals abnormal symmetrically distribute on either side of ellipsoidal CZTSSe with a size of circa 20 nm (Figure 1d). Thus, Au coverage rate ( $R_{\text{Au}}$ ) of CZTSSe is much lower than  $R_{\text{Au}}$  of CZTS. HRTEM micrograph in Figure 1b represents typical growth of Au on CZTS particles, and Figure 1c reveals lattice fringes of the (200) plane of Au and the (312) plane of tetragonal-type kesterite CTZS. Accordingly, Figure 1d-e represent typical growth of Au on CZTSSe particles, and Figure 1f shows lattice fringes of the (200) plane of Au and the (112) plane of CZTSSe.

$\text{Cu}_2\text{ZnSn}(\text{S}_{1-x}\text{Se}_x)_4$ -Au films are employed as counter-electrodes (CEs) for all-solid-state dye-sensitized solar cells. The device structure and SEM image of CZTS-Au CE are shown in Figure 2a and 2b, respectively; detailed fabrication work was reported in our previous work [5]. According to measured  $j$ - $V$  curves (Figure 2c), the power conversion efficiency (PCE) of CZTS-Au (cell-A) is around 4%, which turns to be 43% higher than that of CZTS-Au (cell-B); in other word, solar cells with CZTS-Au CEs exhibit preferable photoelectric conversion performance compared to those with CZTSSe-Au CEs. Besides, a kink behavior is observed for the latter. This can be due to lower  $R_{\text{Au}}$  of CZTSSe and weaker LSPR effects, the hindered charge transportation at perovskite/CE interface slows down hole extraction, and thus imbalanced electron and hole mobility possibly results in the S-shaped  $j$ - $V$  characteristics.

References:

- [1] T. Todorov *et al*, Thin Solid Films **519** (2011), p. 7378.
- [2] M. Xiao *et al*, J. Mater. Chem. A **1** (2013), p. 5790.
- [3] E. Ha *et al*, Adv. Mater. **26** (2014), p. 3496.
- [4] S. Ma *et al*, J. Colloid Interf. Sci. **539** (2019), p. 598.
- [5] S. Ma *et al*, J. Mater. Chem. A **3** (2015), p. 1222.
- [6] This research was supported by the National Natural Science Foundation of China (61604086).

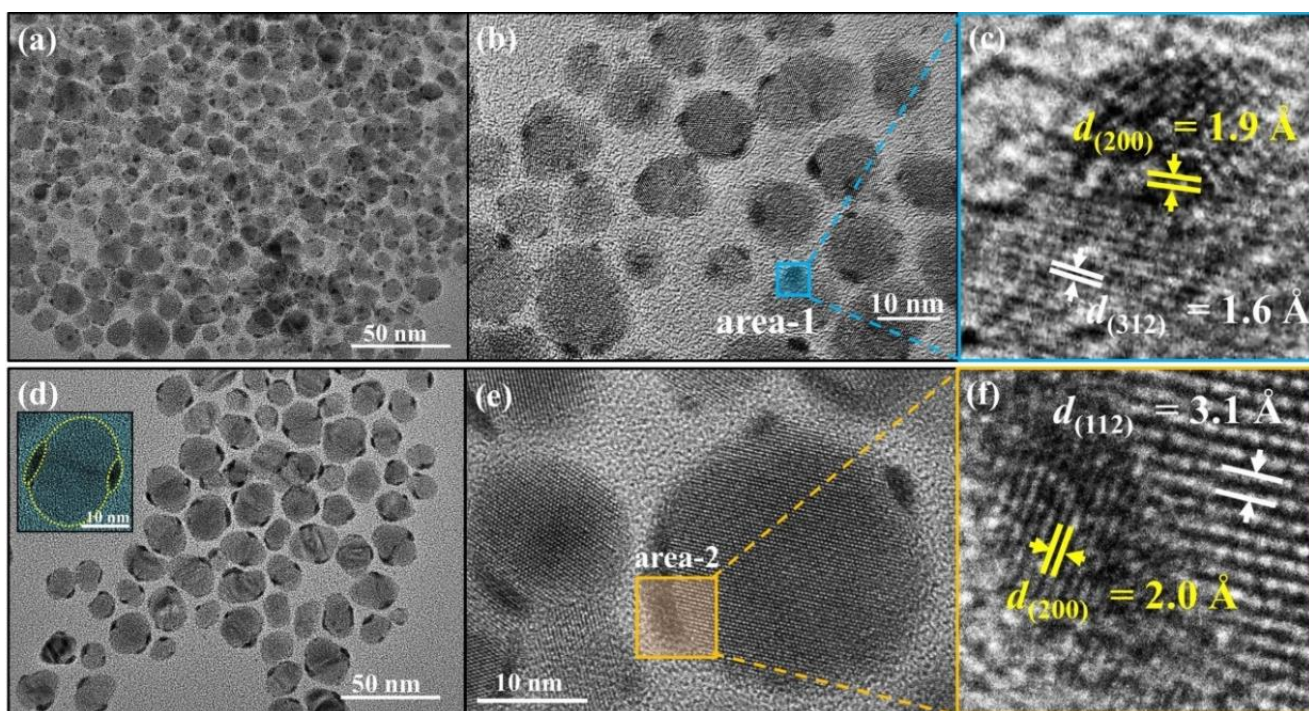


**Figure 1.** (a) TEM image of CZTS-Au. (b) TEM micrograph of CZTS-Au and interfacial structures (c). (d) TEM image of CZTSSe-Au nanoparticles (Inset: a typical symmetrical distribution of Au nanocrystals on ellipsoidal CZTSSe). (e) TEM micrograph of CZTSSe-Au and interfacial structures (f).

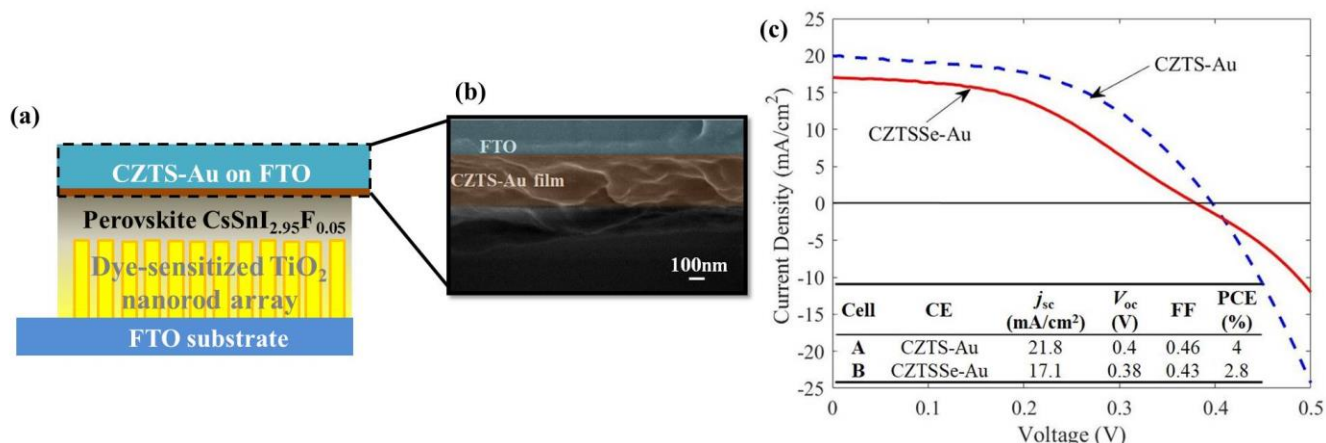


**Figure 2.** (a) Diagram of fabricated solar cell structure with  $Cu_2ZnSn(S_{1-x}Se_x)_4$ -Au CE. (b) SEM image of the cross-section of CZTS-Au on FTO substrate. (c)  $j$ - $V$  characteristics of cell-A and cell-B.